

## Scheme for direct observation of the Wigner characteristic function in cavity QED

M. S. Kim<sup>1,\*</sup>, G. Antesberger,<sup>1,2</sup> C. T. Bodendorf,<sup>1,2</sup> and H. Walther<sup>1,2</sup>

<sup>1</sup>Max-Planck-Institut für Quantenoptik, Hans-Kopfermann-Str. 1, Garching, D-85748, Germany

<sup>2</sup>Sektion Physik, Ludwig-Maximilians-Universität, München, Germany

(Received 14 April 1998)

We suggest a quantum state reconstruction scheme. Our proposal is applicable to the field inside a microwave cavity as well as to the harmonic motion of a trapped atom. It will be shown that the inversion of two-level atoms after a resonant interaction with a coherently displaced quantum state is directly related to the Wigner characteristic function of the initial state. This method neither requires the preparation of atoms in a quantum superposition of the upper and lower energy levels nor heavy numerical processing of the measured data. We demonstrate the reconstruction scheme for the example of a Schrödinger-cat superposition state. [S1050-2947(98)51607-1]

PACS number(s): 42.50.Dv, 84.40.Ik

The reconstruction of quantum-mechanical states for running light fields as well as for cavity fields has been studied extensively in recent times [1]. Quasiprobability distributions and density matrices for running fields have been experimentally determined by the homodyne measurement scheme [2].

Quantum nature does not persist for a long period of time when the nonclassical system is exposed to a classical environment. The quantum state is, thus, better protected in a high- $Q$  cavity [3] or in a trap [4]. Measurement schemes for the field inside a cavity have been proposed by probing the quantum state with two-level atoms and subsequently measuring the atomic subsystem [1,5–9]. Nonclassical motional states of single trapped atoms have already been experimentally reconstructed [10]. The reconstruction scheme requires, however, heavy numerical processing, including using regularization techniques on the measured data.

Despite numerous theoretical suggestions, it is true that the cavity field state has not yet been fully determined by experiment. For convenience, we will therefore confine the discussion to this challenging case, although the suggested method is also applicable to a harmonically bound atom in a trap. We thus focus on the following situation. A single-mode microwave field inside a high- $Q$  cavity is prepared in a well-defined and reproducible (although not necessarily pure) quantum state that shall be investigated. This state is subsequently displaced in phase space by driving the cavity with a strong coherent field. Then the field is probed by a two-level atom, initially prepared in one of its considered energy levels. After a resonant atom-field interaction described by the Jaynes-Cummings model, the atomic inversion is determined by a measurement. The quality factor of the cavity is assumed to be sufficiently large to disregard damping processes in the time period between the preparation of the field and the detection of the atom. The measured probability of atomic inversion for specific interaction times turns out to be the Wigner characteristic function, which is the two-dimensional Fourier transformation of the Wigner distribution. This scheme requires neither the preparation of

atoms in a coherent superposition between upper and lower levels nor heavy numerical processing of the measured data. Moreover, it demonstrates that the Wigner characteristic function can *directly* be measured even though it is a *complex* distribution.

In fact, our scheme is closely related to the nonlinear atomic homodyne detection proposed by Wilkens and Meystre [6,7]. In their setup, an atom is coupled to two modes of the field, one acting as the signal mode, the other as the local oscillator mode. In the present paper we suggest a more realizable scheme based on current experimental conditions.

The displacement of the initial cavity field represented by a density matrix  $\rho$  is carried out by coupling a resonant oscillator to the field mode. In Ref. [9], the oscillator is treated classically. A more complete quantum-mechanical picture is gained by modeling this operation with a beam splitter. The classical oscillator is replaced by a coherent state  $|\gamma\rangle$  and the cavity field is expanded into coherent states  $|\beta\rangle$ , that is,  $\rho = \int P(\beta)|\beta\rangle\langle\beta|d^2\beta$ , where  $P(\beta)$  is the Glauber-Sudarshan distribution [11]. The beam-splitter transformation (see, e.g., Ref. [12]) results in an entangled state of the two output modes. Tracing over one of them yields, for the density matrix  $\rho_D$  of the other mode,

$$\rho_D = D(\sqrt{R}\gamma) \left[ \frac{1}{1-R} \int P\left(\frac{\beta}{\sqrt{1-R}}\right) |\beta\rangle\langle\beta| d^2\beta \right] D^\dagger(\sqrt{R}\gamma). \quad (1)$$

The reflection coefficient  $R$  is determined by the coupling between driving field and cavity. For the case of weak coupling ( $R \approx 0$ ) but still keeping  $\sqrt{R}\gamma \equiv \alpha$  at a finite value—which is the case considered in this paper—the driven cavity field  $\rho_D$  in Eq. (1) is approximated by the unitary transformation  $\rho_D = D(\alpha)\rho D^\dagger(\alpha)$  with the displacement operator  $D(\alpha) = \exp(\alpha a^\dagger - \alpha^* a)$ . Here  $a$  and  $a^\dagger$  are the annihilation and creation operators and  $\alpha = |\alpha|e^{i\phi}$  is a complex number characterizing the amplitude and phase of the *displacement in phase space*.

Now the displaced field state is probed by an atom, injected in its upper level. Assuming exact resonance between atom and cavity field, the Jaynes-Cummings interaction [13]

\*On leave from Department of Physics, Sogang University, C.P.O. Box 1142, Seoul, Korea.

leads to the probability  $p_g$  of finding the atom after the interaction time  $\tau$  in the lower level, which is given by the expression [9]

$$p_g(\alpha, \tau) = \frac{1}{2} - \frac{1}{2} \text{Tr}\{\rho D^\dagger(\alpha) \cos(2\lambda\tau\sqrt{\hat{n}+1}) D(\alpha)\}. \quad (2)$$

The photon-number operator has been denoted by  $\hat{n} = a^\dagger a$ , while  $\lambda$  stands for the dipole coupling strength.

For the remainder of this paper we assume  $|\alpha|^2$  to be large compared to the mean photon number  $\bar{n} = \text{tr}\{\rho\hat{n}\}$  of the initial cavity field. We expand the argument of the cosine function in Eq. (2) into a Taylor series around the average photon number  $\bar{n}_D = \text{tr}\{\rho D^\dagger(\alpha)\hat{n}D(\alpha)\}$  of the shifted state, which can be approximated by  $|\alpha|^2$

$$2\lambda\tau\sqrt{\hat{n}+1} = 2\lambda\tau \left[ \sqrt{|\alpha|^2+1} + \frac{1}{2} \frac{\hat{n}-|\alpha|^2}{\sqrt{|\alpha|^2+1}} - \frac{1}{8} \frac{(\hat{n}-|\alpha|^2)^2}{\sqrt{(|\alpha|^2+1)^3}} + \dots \right]. \quad (3)$$

The large magnitude of the displacement guarantees that the width  $\Delta n_D$  of the photon number distribution will now obey the inequality  $1 \ll \Delta n_D \ll \bar{n}_D$ . Under these circumstances, the Rabi oscillations in the atomic inversion as a function of  $\tau$  show (for a few revival times) well separated collapses and revivals. The first term in the Taylor expansion (3) is the Rabi oscillation, the second term determines the periodical recurrence of collapses and revivals, and the third term modifies the shape of the revivals [14]. In the context of the present paper, we are only interested in the envelope of the Rabi oscillations *before* the first revival, which appears at the scaled interaction time  $\lambda\tau = 2\pi\sqrt{\bar{n}_D}$ . This enables us to take the Taylor expansion only until the second term. Using the relations  $D^\dagger(\alpha)D(\alpha) = 1$  and  $D^\dagger(\alpha)\hat{a}D(\alpha) = \hat{a} + \alpha$ , we find the following approximation for the ground state probability  $p_g$ :

$$P_g(\alpha, \tau) \approx \frac{1}{2} - \frac{1}{2} \text{Re} \left( e^{2i\lambda\tau\sqrt{|\alpha|^2+1}} \times \text{Tr} \left\{ \rho \exp \left[ i\lambda\tau \left( \frac{\hat{n}}{|\alpha|} + a^\dagger e^{i\phi} + a e^{-i\phi} \right) \right] \right\} \right), \quad (4)$$

In Eq. (4),  $\hat{n}/|\alpha|$  can again be neglected by keeping the interaction time sufficiently small compared to the revival time. This finally leads to the following simple result:

$$1 - 2P_g(\alpha, \tau) \approx C_r(\mu) \cos(2\lambda\tau\sqrt{|\alpha|^2+1}) - C_i(\mu) \sin(2\lambda\tau\sqrt{|\alpha|^2+1}). \quad (5)$$

$C_r(\mu)$  and  $C_i(\mu)$  denote, respectively, the real and imaginary parts of the Wigner characteristic function  $C(\mu) = \text{Tr}[\rho D(\mu)]$  for the initial cavity field at the reciprocal phase-space location  $\mu = i\lambda\tau e^{i\phi}$ . The magnitude  $|\mu| = \lambda\tau$

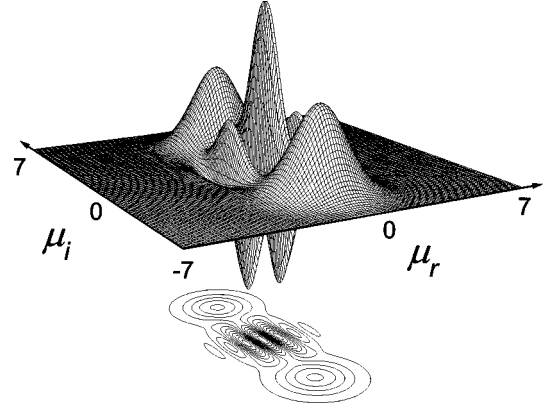


FIG. 1. Wigner characteristic function for a Schrödinger-cat state with the amplitudes  $\zeta = \pm 2i$ . Even though the shape is identical to that of the Wigner distribution, the interpretation of the two Gaussian hills and the oscillations around the origin is just opposite.

equals the scaled interaction time, whereas the angle  $\phi$  is determined by the phase of the driving field. The experimentally observed atomic inversion refers therefore directly to the *real* part of the characteristic function for  $\lambda\tau = n\pi/(2\sqrt{|\alpha|^2+1})$  ( $n=0,1,2,\dots$ ) [this means  $1-2p_g = (-1)^n C_r(\mu)$ ] and to its *imaginary* part for  $\lambda\tau = (n + \frac{1}{2})\pi/(2\sqrt{|\alpha|^2+1})$  [this leads correspondingly to  $1-2p_g = (-1)^{n+1} C_i(\mu)$ ]. Our method enables one to investigate an area of particular interest in the “ $\mu$ -space” without necessarily recording the complete information on the quantum state. Equation (5) implies immediately that the real and imaginary parts of  $C(\mu)$  are bound between  $+1$  and  $-1$ , a well-known property, which is illuminated here in a physical context.

We emphasize that the characteristic function *itself* is a quantum state representation of full value. It is particularly closely related to the momenta of  $a$  and  $a^\dagger$  via its derivatives, that is,  $(\partial/\partial\mu)^n (-\partial/\partial\mu^*)^m C(\mu)|_{\mu=\mu^*=0} = \langle \{a^{\dagger n} a^m\}_{\text{sym}} \rangle$  (sym denotes the symmetrically-ordered product) and to the Wigner distribution via a two-dimensional Fourier transformation. The connection to the density operator is given by the integral transformation  $\rho = \frac{1}{\pi} \int C(\mu) D(-\mu, -\mu^*) d^2\mu$ . In Fock representation, the matrix elements  $\langle n|D(\mu)|m \rangle$  play the role of a *pattern function*.

We exemplify the reconstruction scheme for the cavity field prepared in a quantum-mechanical superposition of two coherent states  $|\pm\zeta\rangle$ , that is,

$$|\psi\rangle = \mathcal{N}(|\zeta\rangle + |-\zeta\rangle), \quad \mathcal{N}^2 = (2 + 2e^{-2|\zeta|^2})^{-1}. \quad (6)$$

The characteristic function for this “Schrödinger cat” can analytically be derived from its definition. In our case (dephasing of  $\pi$ ), the Wigner distribution is inversion symmetric with respect to the origin, and the characteristic function is therefore purely real. It is depicted in Fig. 1 for  $\zeta = 2i$ . When the density matrix satisfies the condition  $\rho_{mn} \equiv 0$  for odd  $m$ , which is true for the coherent superposition state, Eq. (6), the shape of the Wigner distribution and its characteristic functions are *identical*. But note, that in the reciprocal space the interpretation is just the other way

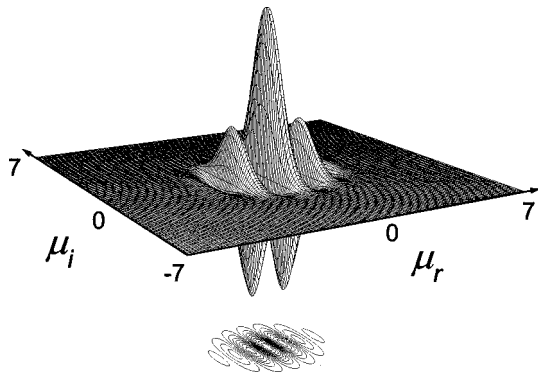


FIG. 2. Wigner characteristic function for a classical mixture of two coherent states with amplitudes  $\zeta = \pm 2i$ .

around: While the two mirror symmetrical Gaussian hills of the Wigner distribution around the amplitudes  $\pm \zeta$  belong to the part that stands for the classical mixture, the hills of the characteristic function are due to the *quantum superposition*; and the oscillations around the origin, which are in the case of Wigner's function well known to display the coherence, belong in terms of the characteristic function to the classical mixture. The characteristic function for the classical mixture of the coherent states  $|\pm \zeta\rangle$  with missing superposition phase information is presented in Fig. 2.

In Fig. 3 we show the atomic inversion according to Eq. (2) for the superposition state, Eq. (6), as a function of the scaled interaction time  $\lambda\tau$  with fixed displacement  $\alpha=10$  (dotted line). The envelope of the fast Rabi oscillations clearly reveals the cut through the characteristic function along the *imaginary axis*  $\mu = i\lambda\tau$  (solid line), as predicted by the analytical approximation, Eq. (5), for  $C_i(\mu) \equiv 0$ . The condition  $\lambda\tau = n\pi / (2\sqrt{|\alpha|^2 + 1})$  for  $C_r(\mu)$ , which is certainly important for the general case [ $C_i(\mu) \neq 0$ ], is marked

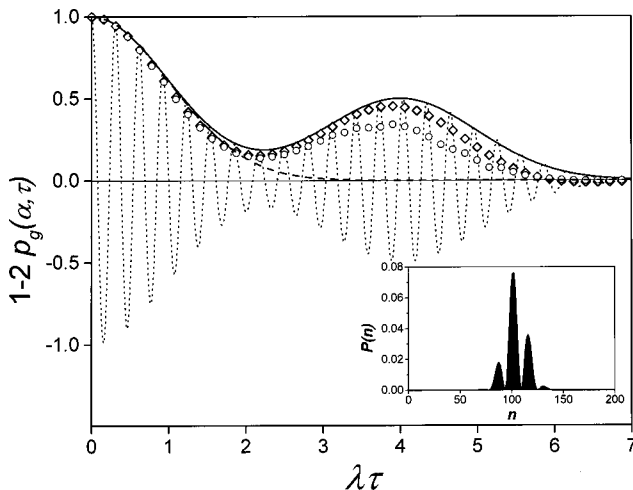


FIG. 3. Comparison between atomic inversion as a function of the scaled interaction time  $\lambda\tau$  (dotted line) and a cut through the Wigner characteristic function  $C(\mu = i\lambda\tau)$  of Fig. 1 along the imaginary axis (solid line) for fixed  $\alpha=10$ . The atomic inversion at the points  $\lambda\tau = n\pi / [2\sqrt{|\alpha|^2 + 1}]$  is marked by rhombuses. An interaction time distribution of  $\Delta\tau/\tau = 1\%$  leads to a lower contrast marked with circles. The dashed line belongs to the statistical mixture of Fig. 2. The inset shows the photon-number distribution of the displaced Schrödinger-cat state.

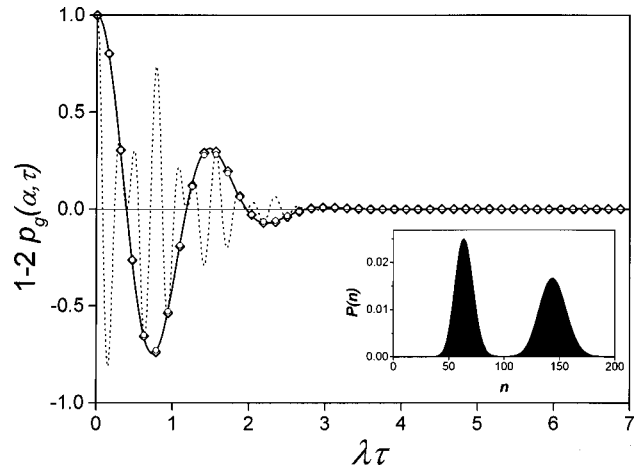


FIG. 4. Same as in Fig. 3 but for  $\alpha=10i$ , which corresponds to a cut through the Wigner characteristic function of Fig. 1 along the real axis.

with rhombuses. We note that the phase of the actual Rabi oscillations differs slightly from that of the approximation (5), which is not surprising, since  $|\alpha|$  is only moderately large. Anyway, the second maximum of the envelope that *indicates the coherence* between the two amplitudes with opposite phases is clearly resolved. This holds also for Gaussian-distributed interaction times with a normalized standard deviation  $\Delta\tau/\tau = 1\%$  (marked with circles), which takes typical experimental errors into account [3,9,15].

The inlay in Fig. 3 shows the photon statistics of the displaced Schrödinger-cat state. The coherence appears as an *interference structure of the photon number distribution*. The energy difference between the single peaks determines the ‘‘satellite revival’’ of the Rabi oscillations. It appears for a much shorter interaction time than the ‘‘real’’ revivals that are due to the energy difference of *directly* neighboring photon numbers (and not included in our approach). The photon statistics of the mixture are simply Poisson-distributed and the envelope of the atomic inversion for this case (dashed curve) reflects the corresponding cut through Fig. 2.

Figure 4 shows the situation for  $\alpha=10i$ , corresponding to a cut through the characteristic function along the *real* axes. The double peaked photon statistics (see inset) belong to the two amplitudes  $\pm \zeta$ . The two associated main frequencies cause the oscillation in the envelope of the Rabi frequency (‘‘beat-signal’’), which again reflects accurately the shape of the characteristic function. The coherent superposition and mixture are indistinguishable for this cut.

In conclusion, we have suggested a scheme to directly measure the characteristic function of a quantum state in a cavity or in a trap at any point in the reciprocal phase space. The method has been demonstrated for a Schrödinger-cat state which can be well distinguished from the corresponding statistical mixture.

We thank Professor Welsch for discussions and for bringing Refs. [6,7] to our attention, Professor Meystre and Dr. Leonhardt for useful discussions, and Dr. Karapanagioti for carefully reading the manuscript. M.S.K. is grateful to the Alexander von Humboldt Foundation and the Korean Ministry of Education for support through Grant No. BSRI-97-2415.

- [1] J. Mod. Opt. **11/12** (1997), special issue on quantum state preparation and measurement, edited by W. P. Schleich and M. G. Raymer.
- [2] K. Vogel and H. Risken, Phys. Rev. A **40**, 2847 (1989).
- [3] O. Benson, M. Weidinger, G. Raithel, and H. Walther, J. Mod. Opt. **44**, 2011 (1997).
- [4] D. M. Meekhof, C. Monroe, B. E. King, W. M. Itano, and D. J. Wineland, Phys. Rev. Lett. **76**, 1796 (1996).
- [5] J. Krause, M. O. Scully, and H. Walther, Phys. Rev. A **34**, 2032 (1986); M. O. Scully *et al.*, *ibid.* **44**, 5992 (1991).
- [6] M. Wilkens and P. Meystre, Phys. Rev. A **43**, 3832 (1991).
- [7] S. M. Dutra, P. L. Knight, and H. Moya-Cessa, Phys. Rev. A **48**, 3168 (1993); S. M. Dutra and P. L. Knight, *ibid.* **49**, 1506 (1994).
- [8] L. G. Lutterbach and L. Davidovich, Phys. Rev. Lett. **78**, 2547 (1997).
- [9] C. T. Bodendorf, G. Antesberger, M. S. Kim, and H. Walther, Phys. Rev. A **57**, 1371 (1998).
- [10] D. Leibfried, D. M. Meekhof, B. E. King, C. Monroe, W. M. Itano, and D. J. Wineland, Phys. Rev. Lett. **77**, 4281 (1996).
- [11] Even though the Glauber-Sudarshan  $P$  function does not behave well for nonclassical field states, it can be used for calculation purposes.
- [12] U. Leonhardt, *Measuring the Quantum State of Light* (Cambridge University Press, Cambridge, 1997).
- [13] For a review, see B. W. Shore and P. L. Knight, J. Mod. Opt. **40**, 1195 (1993).
- [14] N. B. Narozhny, J. J. Sanches-Mondragon, and J. H. Eberly, Phys. Rev. A **23**, 236 (1981); C. Leichtle, I. Sh. Averbukh, and W. P. Schleich, Phys. Rev. Lett. **77**, 3999 (1996).
- [15] M. Brune *et al.*, Phys. Rev. Lett. **77**, 4887 (1996).